Enhancing Visual-Guided Motor Imagery Performance via Sensory Threshold Somatosensory Electrical Stimulation Training

Lei Zhang, Long Chen, Zhongpeng Wang, Xin Zhang, Xiuyun Liu, and Dong Ming, *Senior Member, IEEE*

Abstract*—*Objective: **Motor imagery (MI) based brain-computer interface (BCI) has been widely studied as an effective way to enhance motor learning and promote motor recovery. However, the accuracy of MI-BCI heavily depends on whether subjects can perform MI tasks correctly, which largely limits the general application of MI-BCI. To overcome this limitation, a training strategy based on the combination of MI and sensory threshold somatosensory electrical stimulation (MI+st-SES) is proposed in this study.** ***Methods:*** **Thirty healthy subjects were recruited and randomly divided into SES group and control group. Both groups performed left-hand and right-hand MI tasks in three consecutive blocks. The main difference between two groups lies in the second block, where subjects in SES group received the st-SES during MI tasks whereas the control group performed MI tasks only.** ***Results:*** **The results showed that the SES group had a significant improvement in event-related desynchronization (ERD) of alpha rhythm after the training session of MI+st-SES (left-hand: $F(2,27) = 9.98$, $p<0.01$; right-hand: $F(2, 27) = 10.43$, $p<0.01$). The classification accuracy between left- and right-hand MI in the SES group was also significantly improved following MI+st-SES training ($F(2,27) = 6.46$, $p<0.01$). In contrary, there was no significant difference between the first and third blocks in the control group ($F(2,27) = 0.18$, $p = 0.84$). The functional connectivity based on weighted pairwise phase consistency (wPPC) over the sensorimotor area also showed an increase after the MI+st-SES training.** ***Conclusion and Significance:*** **Our findings indicate that training based on MI+st-SES is a promising way to foster MI performance and assist subjects in achieving efficient BCI control.**

Manuscript received 17 January 2022; revised 25 May 2022 and 28 July 2022; accepted 21 August 2022. Date of publication 29 August 2022; date of current version 20 January 2023. This work was supported by the National Natural Science Foundation of China under Grants 81925020 and 82001939. *(Lei Zhang and Long Chen contributed equally to this work.)* (*Corresponding authors: Long Chen; Dong Ming.*)

Lei Zhang is with the Academy of Medical Engineering and Translational Medicine, Tianjin University, China.

Long Chen is with the Academy of Medical Engineering and Translational Medicine, Tianjin University, Tianjin 300072, China (e-mail: cagor@tju.edu.cn).

Zhongpeng Wang, Xin Zhang, and Xiuyun Liu are with the College of Precision Instruments and Optoelectronics Engineering, Tianjin University, China.

Dong Ming is with the Academy of Medical Engineering and Translational Medicine, Tianjin University, Tianjin 300072, China, and also with the College of Precision Instruments and Optoelectronics Engineering, Tianjin University, Tianjin 300072, China (e-mail: richardming@tju.edu.cn).

Digital Object Identifier 10.1109/TBME.2022.3202189

***Index Terms*—Brain-computer interface (BCI), EEG, motor imagery, sensory threshold somatosensory electrical stimulation.**

I. Introduction

BRAIN-computer interface (BCI) constructs a direct communication pathway between the brain and the external environment, which is particularly beneficial for patients who require neurorehabilitation and motor assistance [1], [2]. In particular, motor imagery based brain-computer interface (MI-BCI) is able to correlate the movement intention and the external afferent signals from assistive devices to promote the recovery of the damaged neural pathways and improve patients' motor performance [3], [4]. As a mental rehearsal of limb movement, motor imagery (MI) can induce neural activations in the sensorimotor cortex, which is similar to actual execution [5], [6]. The neural patterns activated by MI are usually defined as event related desynchronization (ERD) or synchronization (ERS) in alpha and beta rhythm [7], [8]. Theoretically, the ERD patterns should appear steadily when subjects perform motor imagery, but this is not always the case. A large number of subjects are unable to perform MI accurately, which greatly influence their efficiency in using MI-BCI [9].

In the past decades, intensive researches have been conducted to improve the efficiency of MI-BCI. For instance, machine learning algorithms have been greatly improved to enhance the capability of MI patterns detection. The Common Spatial Pattern (CSP), as one of the most widely used algorithms, is able to distinguish MI patterns efficiently by constructing spatial filters [10]. In addition to traditional algorithms, deep learning algorithms become popular and are also introduced in MI-BCI [11]. These advanced algorithms significantly improve the decoding performance of MI-BCI.

Despite these advances, the application of MI-BCI is still limited, in part due to the poor quality of EEG signals produced by subjects who are unable to perform the MI tasks properly [12], [13]. Therefore, many researchers have turned their attention to the subject training process. The neurofeedback training has been integrated into the MI-BCI system to train subjects to self-regulate neural responses. Bhattacharyya et al. demonstrated that functional electrical stimulation (FES) feedback-based BCI is more effective than visual feedback-based BCI in improving

participants' motor imagery learning [14]. Wang et al. designed a haptic-visual feedback-based BCI system and they demonstrated that neurofeedback training improved sensorimotor cortical activations and classification performance [15]. However, the efficiency of neurofeedback-based BCI still depends on whether the initial classifier is able to produce accurate feedback signals, or else, it may play a negative role [16], [17]. The accuracy of initial classifier, which is trained offline in the calibration process, heavily relies on the quality of neural signals generated when subjects perform MI tasks. Therefore, it is necessary to develop appropriate MI guidance strategies to help subjects execute MI tasks effectively and correctly. Some studies suggested that VR system is able to improve the performance of MI via direct visual guidance and increased subject involvement [18], [19]. In addition, somatosensory afference, which is crucial to build the mental representation necessary for MI, has also received greater attention recently. Shu et al. demonstrated that the recognition accuracy of MI patterns is enhanced when a vibrotactile stimulation is provided concurrently during MI [20]. Corbet et al. found that the combination of MI and sensory threshold somatosensory electrical stimulation (st-SES) increases connectivity between the frontal and parietal networks [21]. Similar results were also reported by Vidaurre et al. [22]. However, for some participants, the somatosensory afference guidance may direct participants' attention away from MI tasks and toward external sensory stimulation. Additionally, some types of somatosensory afference may induce ERD patterns similar to that during MI, which possibly generate a bias in the analysis of neural responses elicited by MI. It is uncertain whether the enhancement of ERD patterns is induced by MI performance or somatosensory stimulation. Therefore, some studies have explored the after-effects of somatosensory afference guidance on cortical activation [23], [24]. Yao et al. proposed a vibrotactile stimulation training approach to improve the performance of BCI based on somatosensory attentional orientation (SAO) [24]. In the SAO task, subjects were asked to imagine tactile sensation induced by the vibrotactile stimulation. Although subjects achieved better SAO-BCI accuracy after sensory stimulation training, SAO-BCI did not purely discriminate the motion intention of different hands. At present, many studies have shown that MI has unique advantages in the fields of motor learning and neurorehabilitation. However, the role of SAO in the above fields remains to be determined. Recently, an ingenious training strategy based on alpha frequency intervention was developed by Zhang et al. to enhance the classification performance of MI-BCI [23]. In that work, the difference in alpha band power between left- and right-hand MI tasks increased after applying alpha frequency electrical stimulation to the ulnar nerve of the contralateral hand relative to the imagined hand. These findings suggest that training strategies based on peripheral stimulation can modulate cortical activity and affect BCI performance. However, the brain patterns detected after peripheral stimulation-based training may be caused by carry-over effect of the stimulation itself rather than induced by improved MI performance. Therefore, it would be interesting to investigate whether the subject's MI performance could be improved after somatosensory afference without interference from carry-over effect of somatosensory stimulation.

As an effective tool to convey the proprioceptive sensation by depolarizing sensory nerve, st-SES has been suggested to be a useful tool for facilitating cortical activity without inducing detectable ERD brain patterns [21]. Therefore, we conducted the current study to test the effect of st-SES as a training tool on MI tasks. In particular, the frequency of st-SES in this study was outside the frequency range of sensorimotor rhythm of interest (8-30 Hz) to avoid the potential carry-over effect of st-SES itself. We hypothesized that the training via the combination of MI and st-SES (MI+st-SES) would improve subjects' performance on MI tasks. Therefore, we expected that there was an improvement of MI-BCI classification accuracy and sensorimotor cortical activation after MI+st-SES training.

II. Methods

A. Participants

Thirty right-handed healthy subjects with normal or corrected to normal vision, participated in the experiment (average age 24.3 ± 1.1 years). The study was approved by the ethical committee of Tianjin University. Written consent form was obtained from each subject. The subjects were randomly divided into SES group and control group, with fifteen subjects in each group.

B. EEG Recording and St-SES Intervention

EEG data were recorded using SynAmps2 system (Neuroscan, Victoria, Australia) with 60 standard Ag/AgCl electrodes in a 10-10 standard configuration (Fig. 1(b)). The reference electrode was placed on nose and the ground electrode was on the forehead. EEG signals were sampled at 1000 Hz with a notch filter at 50 Hz to filter out power line noise. The impedances were kept under 10 kΩ during the data acquisition process.

St-SES was generated using a portable electrical stimulation device called Rehastim 2 (Hasomed, Magdeburg, Germany). The electrodes were placed on the flexor digitorum superficialis at the anterior face of the forearms. The frequency of stimulator was set to 40 Hz for all participants. This frequency is above the range of sensorimotor rhythm (from 8 to 30 Hz) of interest. The stimulation amplitude of st-SES was individually evaluated for each participant. The amplitude was gradually increased from 0mA until a sensation of hand closure was reported by the participant, while the amplitude was adjusted to avoid eliciting any visible movement. The stimulation intensity varied between 3 to 5 mA according to participant-dependent sensory threshold.

C. Design of the Experimental Paradigm

The experimental procedures were similar in both groups. During the setup process, all subjects were instructed to clench left hand (LH) fist or right hand (RH) fist in order to familiarize themselves with the proprioceptive sensations. After that, all groups performed three blocks of motor imagery, with 10-min rest between blocks to avoid mental fatigue. In order to ensure that subjects imagined actions exactly as prescribed, action observation was used to provide content and cues for motor imagery [25]. During MI, subjects received guidance via visualization of a hand clenching movement. Both groups

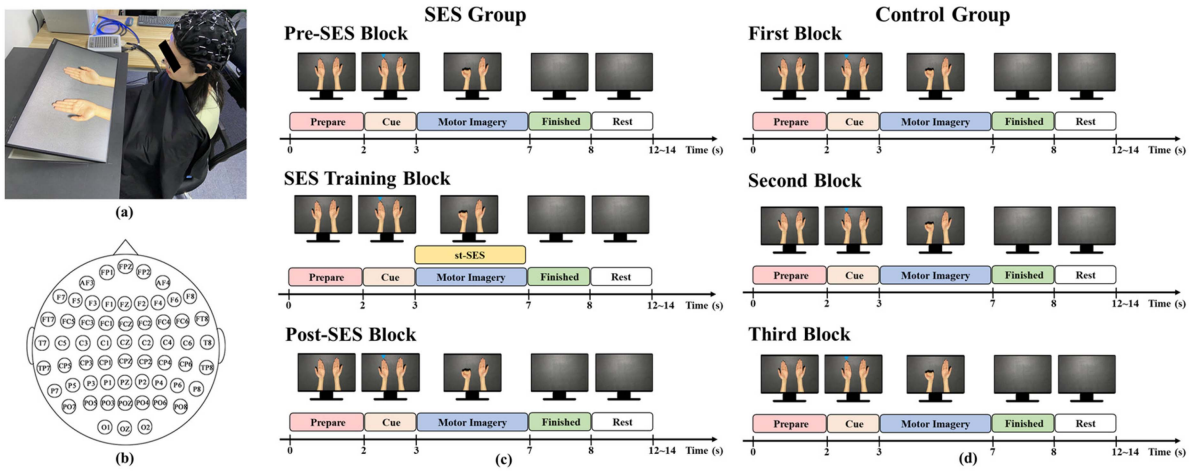

Fig. 1. Experimental paradigm. (a) A visual representation of the experimental scene. (b) Electrodes placement according to the standard 10-10 system. (c) The experimental procedure of three blocks in SES group. In each trial of pre-SES and post-SES block, subjects were required to perform motor imagery tasks according to the cue. In each trial of SES training block, st-SES was given to subjects during MI tasks. (d) The experimental procedure of three blocks in control group.

completed the same tasks in the first and third blocks. In the second block, the SES group executed the MI training tasks with st-SES application, whereas the control group executed the MI training tasks alone. For the control group, the stimulation electrodes were also placed on the flexor digitorum superficialis of the forearms. The subjects in the control group were informed that electrical stimulation was applied to the forearm during the MI training tasks, but the stimulation amplitude was small and imperceptible. In fact, the electrical stimulation device was turned off during the MI training tasks in the control group. The experimental protocols of three blocks are illustrated in Fig. 1 and organized as follow:

The first block (pre-SES block for SES group). As shown in Fig. 1(c) and (d), at the beginning of each trial, a pair of model hands appeared in the center of the screen for 2 seconds to alert participants to get ready for the MI task. Then, a cue triangle randomly appeared on either the left or right model hand to indicate which hand movement to imagine. This cue lasted for 1 s, followed by a corresponding hand clenching presented on the screen for 4 s. In this period, subjects were asked to perform kinesthetic imagery of hand closure movement without causing muscular contraction. In addition, subjects were instructed to focus on the performance of MI task rather than the model hands presented on the screen. The task was finished once the model hands disappeared. The inter-trial intervals varied randomly between 4 and 6 s to prevent adaptation. This block included four runs, with each run performing 20 trials (i.e., 10 trials for each side).

The second block (SES training block for SES group). The trial timing and the cues in the second block were similar to the first block. For the SES group, the st-SES was applied to the participants' corresponding forearm during MI task. As shown in Fig. 1(c), in each trial, st-SES was triggered at the beginning of MI task and lasted for 4 s. For the control group, the participants were required to perform MI tasks without the activation of st-SES. A total of 80 trials with 40 trials for each side were completed by the subjects in four runs.

The third block (post-SES block for SES Group). The experimental paradigm of each trial in the third block was identical to the first block. Participants performed four runs of MI tasks with 40 trials at each side.

During the experiment, participants were instructed to sit in a relaxed position in front of the screen, with their elbows flexed at 90° and their hands supinated in a comfortable position under the table. The display was placed horizontally to the table with a 15-degree slant (Fig. 1(a)) to guarantee that the participant's hands and the observed hands were anatomically and perceptually identical. During task period, the participants were required to restrict their movements, such as blinking or swallowing, which may produce artifacts.

D. Time–Frequency Analysis

EEG signals were firstly band-pass filtered into 1 to 100 Hz, then down sampled to 250 Hz. Noisy channels (detected by visual inspection) were substituted by the mean of the orthogonal neighboring channels [21]. Independent component analysis (ICA) was then used to filter out ocular and electromyogram artifacts from the EEG signals. The rank-deficiency problem was accounted by reducing the number of ICs. Spherical spline Laplacian, also referred to as current source density (CSD), was then applied to transform EEG signals into estimates of radial current flow at scalp. This was done according to Perrin et al.'s method [26], as implemented in the CSD toolbox [27]. After that, the artifacts on the EEG signals were manually removed by using EEGLab toolbox [28]. Trials contaminated by artefacts were marked as artifactual and then discarded in analysis. In each block, at least 36 trials for both the LH MI task and the RH MI task were reserved for further analysis.

In order to evaluate the effect of SES training on brain activity, we compared event-related spectral perturbation (ERSP) among three blocks in both SES group and control group. ERSP has been widely used to describe power changes of EEG signals in time-frequency domain. In a defined frequency band, the

increase or decrease of power relative to baseline can be represented in the form of ERS or ERD. The calculation formula of ERSP for n trials was defined as follow:

$$ERSP\,(f,t) = \frac{1}{n}\sum_{k=1}^{n} F_k(f,t)^2 \tag{1}$$

where F_k (f, t) represents the spectral estimation of kth trial at frequency f and time t. The short-time Fourier transform (STFT) with Hanning-tapered window from EEGLab was applied to compute the ERSP (dB). The baseline period was set between 0.2 and 1 second before the appearance of model hands (from -1 to -0.2 s). The ERSP values were then normalized by subtracting the mean power during baseline period.

The ERSP analysis were carried out by extracting the power changes for time period from -2 to 8 s and frequency bands of 3–35 Hz. This frequency band of interest overlapped with sensorimotor rhythms. The values of ERSP at contralateral key channel (i.e., C4 for LH task and C3 for RH task) were analyzed for each task. In order to quantify the ERD patterns, the relative ERD values were calculated as the average power spectrum at baseline subtracted from average power spectrum during the task period and divided by the average baseline power spectrum. A statistical analysis was performed to evaluate the effect of MI+st-SES based training on the relative ERD values in two frequency bands separately (alpha: 8–13 Hz, beta: 14–30 Hz).

For topographical analysis, the ERSP values of each electrode were averaged across task period and across alpha and beta frequency bands to obtain spatial distribution of cortex activation. The cluster-based permutation test was used to compare the topographical patterns between the first and third blocks in each group. The threshold used to determine significance electrode clusters was set to 0.05 ($p < 0.05$). In order to identify possible anatomical regions of significant topographical differences between pre-training block and post-training block, the ERSP differences obtained in sensor space were projected to source space. First, a boundary element head model was created based on the Montreal Neurological Institute (MNI) brain template, and EEG channels were overlaid onto the scalp surface of this head model. The cortical mesh surface obtained from the MNI template had 20173 voxels and was then used to construct a source model. After that, leadfield matrix was calculated based on the head model and source model. Exact low resolution brain electromagnetic tomography (eLORETA) was used to generate the spatial filter to correlate scalp-level and source-level activity. This spatial filter was then used to project ERSP differences of significant electrode clusters to the source space.

Furthermore, we calculated coefficient of determination r^2 to evaluate the differences of EEG signal spectra between LH and RH tasks for each block. The r^2 value can be between 0 and 1, with r^2 value close to 1 indicating a good discrimination of both MI tasks and r^2 value close to 0 indicating that the MI tasks can be distinguished very scarcely [29]. Here, r^2 value of each channel was calculated in the frequency band of [8, 30] Hz and timing interval of [3, 7] s for each subject. In each channel, subjects with the r^2 values more than three scaled median absolute deviations (MAD) away from the median were considered outliers and were excluded from calculation of the mean r^2 values. The function isoutlier.m in Matlab R2020 (The MathWorks, Inc., Natick, Massachusetts, United States) was applied to detect outliers.

E. Feature Extraction and Classification

Prior to the feature extraction, raw EEG data were band-pass filtered between 8 and 30 Hz and down sampled to 250 Hz. Then, the trials were epoched within the task period from 3 to 7s. After that, the common spatial pattern (CSP) algorithm was applied to extract EEG features. The CSP is a supervised method that maximizes the variance difference between two classes to extract discriminative spatial features from EEG. The first and last four log variance features were chosen as feature vectors. These features were then used to train a linear support vector machine (SVM) classifier to discriminate LH MI task from RH MI task, with the regularization parameter C of classifier set to the default value of 1. The performance of classifier was evaluated through 10 $\times$ 10-fold cross-validation method for each block. The 80 trials in each block were randomly divided into forty sets, with each set including a LH MI sample and a RH MI sample. At each round of 10-fold cross validation, forty sets were randomly decomposed into ten equally sized distinct partitions. At each fold, one partition was used for testing and the remaining partitions were used to train the classifier. This resulted in 10 different accuracies, which were then averaged. In order to avoid possible severe overfitting, CSP filters were calculated repeatedly on the training set within each fold [30]. The same round was repeated 10 times and the final classification performance of each subject was evaluated with the average of all round classification accuracies. Note that the real chance level depends on the classifier and the number of trials. According to the recommendation of Müller-Putz et al., the chance level of accuracy was set as 0.60 [31].

F. Functional Connectivity Analysis

To understand the impact of MI+st-SES training at brain network level, weighted pairwise phase consistency (wPPC) was used to compute functional connectivity between brain areas. wPPC is a method to estimate the consistency of phase angles between trial pairs and it is independent of the number of trials, making it unbiased even the trial pool is small [32]. Due to the high-pass filtering may introduce dependencies among neighboring data samples, it is not used for connectivity analysis. Prior to the wPPC calculation, raw EEG were low-pass filtered below 100 Hz. The data trends were then remove by piecewise-linearly detrending using a 330 ms window every 82.5 ms. As described in the time-frequency analysis section, the pre-processing for functional connectivity analysis also included artifacts removal via visual inspection, ICA and surface Laplacian, etc.

EEG data of 30 channels, including F line channels (F1∼F6), FC line channels (FC1∼FC6), C line channels (C1∼C6), CP line channels (CP1∼CP6) and P line channels (P1∼P6), were selected to construct wPPC functional network. These 30 channels are overlying motor related cortical areas. The wPPC was then calculated using the function ft_connectivity_ppc.m implemented in the Fieldtrip toolbox [33]. The larger the wPPC value,

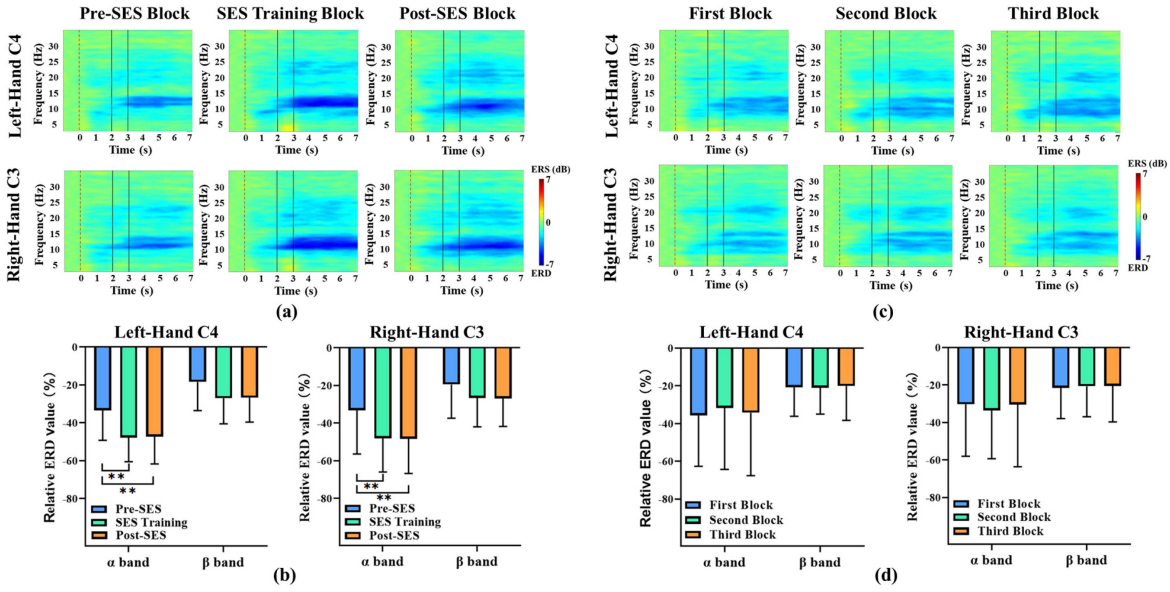

Fig. 2. Time-frequency analysis of contralateral key channel in the SES group and the control group. (a) Grand averaged time-frequency maps of ERSP values for the three blocks in the SES group. The period [3, 7] s indicates the MI tasks. The time window [0, 2] s corresponds to prepare phase and period [2, 3] s corresponds to cue phase. (b) Averaged ERD values over contralateral sensorimotor cortex in the SES group. The ERD values were averaged in the time segment of [3, 7] s and in the frequency band of alpha (8–13 Hz) and beta (14–30 Hz). (c) Grand averaged time-frequency maps of ERSP values for the three blocks in the control group. (d) Averaged ERD values over contralateral sensorimotor cortex in the control group. Error bars represent the standard deviation. '$**$' indicates $p < 0.01$.

the greater the phase consistency between channels. Here, wPPC values were calculated from EEG data within task period of [3, 7] s. After that, the wPPC values in each paired channels were normalized by subtracting the mean wPPC value of baseline period [-1, -0.2] s and divided by the standard deviation of wPPC value during baseline period. Then, the statistical significance of non-zero wPPC values was determined using a permutation test based on the t-statistic (5000 permutations). The maximum statistic test was applied to correct for multiple comparisons and the statistical threshold was set at 0.05. Functional connectivity analysis was performed across all subjects in the pre-SES and the post-SES blocks respectively.

G. Statistical Analysis

Furthermore, relative ERD values and classification accuracies were analyzed using mixed design 2 × 3 ANOVA with group (SES group, control group) as a between-subjects factor and block (first block, second block and third block) as a within-subjects factor. A significant interaction was followed up by simple effects tests of block for each group to test for significant changes in performance over blocks. Bonferroni correction based on multiple comparisons was used for post-hoc tests when the simple effects of block were determined to be significant.

III. Results

A. Task-Related Desynchronization

As shown in Fig. 2(a) and (c), a clear ERD was observed in alpha and beta rhythms for all three experiment blocks during MI task period in both groups. The ERD was stronger during SES training block compared to the initial block in the SES group. Moreover, the MI+st-SES based training seems to be able to improve subjects' MI performance, demonstrated by stronger ERD in the third block (post-SES) than the first block (pre-SES) in SES group. However, this difference is not observed in the control group.

Furthermore, a 2 × 3 (group × block) mixed design ANOVA revealed a significant group by block interaction for relative ERD values in alpha rhythm, regardless of LH ($F(2,56) = 6.44$, $p<0.01$) or RH tasks ($F(2,56) = 3.7$, $p = 0.031$). Tests of simple effects revealed that relative ERD values in alpha rhythm were significantly different among three blocks in the SES group for both LH ($F(2,27) = 9.98$, $p<0.01$) and RH tasks ($F(2,27) = 10.43$, $p<0.01$). Bonferroni post-hoc tests for alpha rhythm highlighted that the relative ERD values were significantly smaller in post-SES block compared with pre-SES block in both LH ($p<0.01$) and RH tasks ($p<0.01$) (Fig. 2(b)). In addition, relative ERD values were also significantly smaller in SES training block than in pre-SES block during the LH ($p<0.01$) and RH ($p<0.01$) tasks. No significant changes were observed in the relative ERD values of alpha band between SES training block and post-SES block. In the control group, tests of simple effects indicated that there was no significant change in relative ERD values of alpha band, regardless of LH ($F(2,27) = 0.65$, $p = 0.533$) or RH tasks ($F(2,27) = 0.5$, $p = 0.612$) (Fig. 2(d)). For relative ERD values in beta rhythm, a 2 × 3 (group × block) mixed design ANOVA revealed no significant interaction between group and block in both LH ($F(2,56) = 2.97$, $p = 0.059$) and RH tasks ($F(2,56) = 2.69$, $p = 0.077$). In addition, there was no significant main effect of group (LH: $F(1,28) = 0.48$, $p = 0.494$; RH: F(1,28)

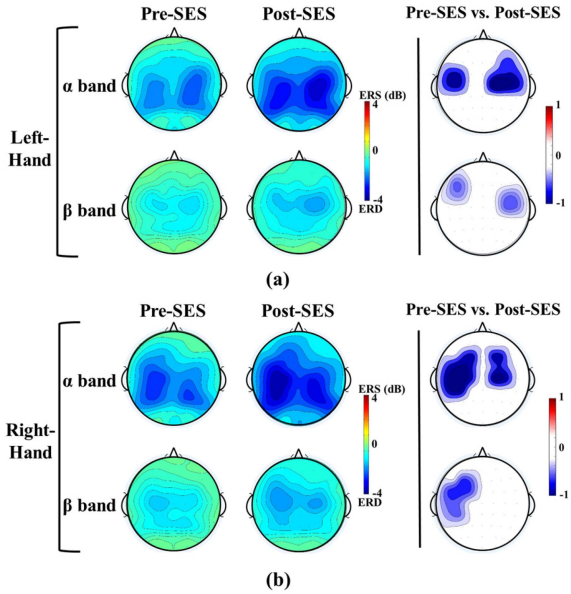

Fig. 3. Comparison of topographical activation patterns between pre-SES block and post-SES block. (a) Averaged spatial distributions of ERSP values in the left-hand MI tasks. (b) Averaged spatial distributions of ERSP values in the right-hand MI tasks. The depicted ERSP values are averaged in the time segment of [3, 7] s and in the frequency band of alpha (8–13 Hz) and beta (14–30 Hz). The pre-SES vs. post-SES maps show the significant ERSP differences between pre-SES and post-SES blocks.

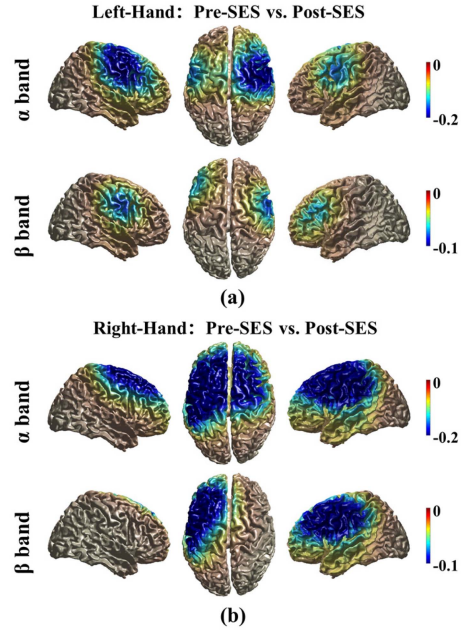

Fig. 4. Source-localized brain maps of significant topographical differences between pre-SES and post-SES blocks. (a) Source-localized brain maps in left-hand MI tasks. (b) Source-localized brain maps in right-hand MI tasks.

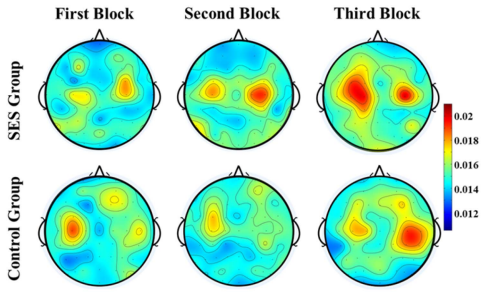

Fig. 5. Grand-averaged topography of r^2 values across different blocks and groups.

$= 0.36$, $p = 0.552$) or block (LH: $F(2,56) = 2.84$, $p = 0.067$; RH:$F(2,56) = 1.58$, $p = 0.216$) on relative ERD values of beta band. The unpaired t-test confirmed that there was no significant difference in relative ERD values in the first block between the SES group and the control group, regardless of LH (alpha: $t(28) = 0.28$, $p = 0.783$; beta: $t(28) = 0.41$, $p = 0.683$) or RH tasks (alpha: $t(28) = -0.3$, $p = 0.766$; beta: $t(28) = 0.33$, $p = 0.743$).

The topographical distribution maps for pre-SES and post-SES blocks in SES group are presented in Fig. 3. For the LH tasks, the ERD was more pronounced on the right hemisphere in both alpha and beta rhythms. Whereas, for the RH tasks, the ERD was stronger on the left hemisphere. In alpha rhythm, the statistical analysis showed that the ERD pattern in bilateral sensorimotor cortex was significantly stronger in the post-SES block compared to the pre-SES block. In beta rhythm, the topographical differences mainly appeared in the contralateral sensorimotor cortex and ERD pattern was stronger in the post-SES block compared to the pre-SES block. No significant topographical difference was found between the ERD patterns of the first and the third blocks in the control group, no matter which tasks (LH or RH) were performed.

The source-localized maps of the SES group showed that the significant differences of ERD pattern in alpha rhythm during LH MI tasks were related to neural activity changes of several brain regions, including bilateral primary motor cortex (M1), bilateral primary somatosensory cortex (S1) and bilateral premotor cortex (PMC) (Fig. 4(a)). Besides the above regions, the st-SES application during the RH MI tasks also influenced the left somatosensory association cortex and bilateral dorsolateral prefrontal cortex (DLPFC) (Fig. 4(b)). On the contrary, ERD in beta band during LH tasks was pronounced in right M1, right S1, right PMC and left DLPFC, and ERD in beta band during RH tasks was significantly increased in left M1, left S1, left PMC, left somatosensory association cortex and left DLPFC regions.

Fig. 5 shows the spatial distribution of averaged r^2 values across different blocks and groups. For each block, no more than four extreme outliers were excluded from each channel. The topographies of the r^2 values revealed the difference in discriminative information distribution across experimental blocks. For the SES group, the r^2 values of post-SES block were greater than those of pre-SES block. Moreover, the increase in r^2 values for post-SES block was mostly focused in the vicinity of channels C3 and C4, implying that sensorimotor cortex was modulated by the MI+st-SES training. For the control group, the r^2 values of the third block did not show consistent changes in both hemispheres compared to the first block.

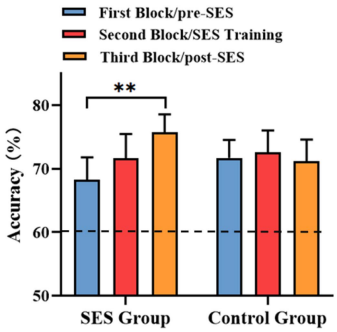

Fig. 6. The classification accuracies for three blocks in SES Group and Control Group. Error bars represent standard error of mean. '**' indicates $p < 0.01$.

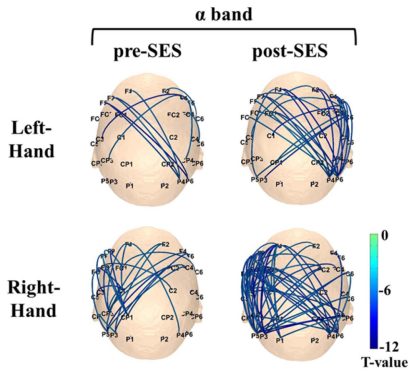

Fig. 7. Statistical contrast maps of functional connectivity between motor imagery and resting states in pre-SES and post-SES blocks. The line in maps represents the significant connectivity.

B. Classification Accuracy

The accuracy of SVM classifier in different experimental blocks are presented in Fig. 6. The classification accuracies above chance level (60%) indicated the ability of distinguishing MI patterns between LH and RH tasks. For classification accuracies, a 2 × 3 (group × block) mixed design ANOVA revealed a significant group by block interaction ($F(2,56) = 3.32$, $p = 0.044$). Simple effects analysis found that there was a significant difference in accuracy among the three blocks in SES group ($F(2,27) = 6.46$, $p<0.01$). Bonferroni post-hoc comparison showed the average accuracy of post-SES block was significantly improved after the MI+st-SES training compared with the accuracy of pre-SES block (75.68±11.06% vs. 68.25±13.66%, $p<0.01$, Fig. 6). The average accuracy of SES training block was higher than that of pre-SES block, yet this difference was not significant (71.66±14.63% vs. 68.25±13.66%, $p = 0.455$). In addition, no significant difference in accuracy was found between SES training block and post-SES block ($p = 0.289$). For control group, tests of simple effects revealed that there was no significant difference in the classification accuracy among the three block (71.69±10.978%, 72.58±13.27% and 71.18±13.21% for the three blocks, respectively, $F(2,27) = 0.18$, $p = 0.84$). The unpaired t-test did not find significant difference in average accuracy in the first block between the SES group and the control group ($t(28) = -0.76$, $p = 0.453$).

C. Functional Connectivity Results

At the brain network level, functional connectivity alterations between MI and resting state could be observed in both pre-SES and post-SES blocks (Fig. 7). These network connectivity changes involved both intra-hemispheric and inter-hemispheric interactions. In the alpha rhythm, the lateralization of the network could be clearly observed in the contralateral hemisphere when the subjects performed the MI tasks. Additionally, the number of functional connections in post-SES block was much higher than that in pre-SES block. Notably, we detected significant decrements of phase consistency at alpha band during the MI state compared to the resting state. For the beta rhythm, there was no significant difference in the functional connectivity between MI and resting state.

IV. Discussion

In the present study, we investigate the effect of a training strategy for MI performance improvement based on MI and st-SES. The results showed that combining MI with st-SES can enhance neural response patterns during MI tasks and improve the accuracy of classifier.

A. Enhancement of Neural Activation

Previous studies have demonstrated that somatosensory stimulation during MI increases sensorimotor cortical activation intensity [21], [22]. The results of this study further validated that the motor-related cortical excitability was consistently improved following MI+st-SES training intervention. As demonstrated in time-frequency analysis, alpha and beta desynchronization in the contralateral sensorimotor cortex was similar among three blocks in control group. By contrast, the ERD patterns of alpha and beta rhythm were larger in the post-SES block compared with the pre-SES block in the SES group. Specially, desynchronization in alpha rhythm was significantly larger after MI+st-SES training, even though st-SES was not provided in the post-SES block. Therefore, the enhancement of ERD in the post-SES block can only be explained by the MI+st-SES training, not by subjects' increased proficiency on the tasks over time of participation. Additionally, in order to reduce the effect of somatosensory stimulation itself on the sensorimotor cortex, st-SES was used as a training tool to improve MI performance in this study. Previous researches have showed that st-SES alone does not induce detectable ERD over the sensorimotor cortex [21], [22]. Thus, the changes in the brain patterns detected after MI+st-SES training were due to an improvement in MI performance rather than a carry-over effect of st-SES itself.

The enhancement of ERD patterns in SES training block could be explained by the fact that the kinesthesia illusion evoked by st-SES strengthened proprioceptive afference related to MI tasks [34]. Recent evidence has shown that proprioceptive afference may play an important role in the formation of body representation and the improvement of neural activation [21]. Thus, by providing proprioceptive afference, st-SES may help to promote the activation of sensorimotor cortex during MI. In addition, we also observed an improvement of ERD patterns in

post-SES block, even though st-SES is no longer present. One possible interpretation of this result is that the memory related to somatosensory sensations may still be preserved after the st-SES intervention. Indeed, proprioceptive afference contributes to the recall of motor memory, and the recruited motor memory is beneficial to the maintenance of prior sensory information [35]. This could explain the similar ERD patterns we observed in SES training and post-SES blocks.

Another potential reason for improvement of ERD patterns in SES training block is neuroplasticity changes caused by the MI combined with st-SES. Indeed, Stefan et al. have shown that conjoint activities of motor cortical circuits and somatosensory afferents could induce the changes in motor cortical excitability [36]. Takahashi et al. have also suggested that the combination of MI and electrical stimulation increases corticospinal excitability [37]. Thus, the combination of intrinsic sensorimotor cortical activity during MI and ascending sensory pathway activation produced by st-SES may induce long-term potentiation in somatosensory cortex. According to these findings, the enhancement of motor-related cortical excitability in post-SES block may also be interpreted as the neuroplasticity changes caused by MI+st-SES based training intervention.

In the statistical analysis of relative ERD values, it was shown that there was a significant interaction between group and block on the ERD patterns only in the alpha band, but not in the beta band. Although, a reduction in oscillatory power in both alpha and beta bands corresponds to the disinhibition of the sensorimotor cortex, alpha and beta rhythms may play distinct roles during MI. The modulation of alpha band power reflects general activation of motor systems with a widespread cortical distribution, whereas beta band is associated with coherence between the sensorimotor cortex and muscles [38], [39]. In the present study, since st-SES was only applied to participants during the SES training block, cortical-peripheral communication may not have changed significantly across three blocks. Therefore, no significant group by block interaction be found in ERD patterns of beta band. Nonetheless, there was a trend for larger beta band ERD in the post-SES block compared with the pre-SES block. It would be interesting to investigate changes in corticospinal excitability following MI+st-SES training in future studies.

The topographical distributions analysis showed that bilateral ERD patterns in alpha band were greater in the post-SES block than in the pre-SES block. However, the sensorimotor cortical ERD differences between pre-SES and post-SES blocks in the beta band were only identified in the contralateral hemisphere. These results are consistent with the previously mentioned interpretation that alpha and beta rhythms may play different roles during MI. In contrast to the relatively widespread desynchronization of alpha rhythm in sensorimotor related regions, the beta rhythm modulation is more restricted to the corresponding somatotopic representation areas [40]. Notably, the left DLPFC was more activated in the post-SES block during both left- and right-hand MI. Indeed, Foerster et al. have shown that transcranial direct current stimulation over left DLPFC can increase the neuroplastic effects of motor imagery on motor learning [41]. Therefore, the increased cortical activation may be an indirect reflection of the enhanced MI performance.

B. Improvement of Classification Performance

The classification accuracy is critical in guaranteeing the effective application of BCI. Therefore, many studies have been devoted to improving the classification performance of MI-BCI. Zhang et al. showed that alpha frequency electrical stimulation is an effective training strategy to enhance MI-BCI performance by regulating the mu-rhythm [23]. Unlike Zhang et al., who used electrical stimulation on the contralateral hand relative to the imagined hand to modulate the pattern of mu-rhythm power, we applied st-SES to the subject's corresponding imagined hand to guide subject during MI. Moreover, we set the frequency of st-SES to 40 Hz in this study to prevent the interference from the carry-over effect of st-SES on subsequent neural response analysis.

In the current study, the classification accuracy was improved by 7.4% after the MI+st-SES training in the SES group. In contrast, there was no significant difference in classification performance between the first and third blocks in the control group. The superior classification accuracy obtained in post-SES block might be attributed to the greater differences in brain activation patterns of MI tasks induced by training intervention based on st-SES and MI. This interpretation is consistent with the results that the r^2 values over the sensorimotor areas were larger in post-SES block than in pre-SES block. The difference in r^2 values indicated that the electrophysiological features of different MI tasks in the post-SES block could be more easily distinguished, which was beneficial to classification performance. However, we also observed that the decoding accuracy of SES training block was not significantly higher than that of pre-SES block. This finding is inconsistent with previous studies in which the MI-BCI performance can be improved by guidance modality based on sensory stimulation [20], [21]. The deviation of the results may be due to the difference in the neural patterns utilized to train the BCI classifier. Previous studies built classifiers to discriminate MI from resting state, whereas the classifiers in this work were trained to distinguish between the left-hand MI and right-hand MI. Indeed, Vidaurre et al. also demonstrated that sensory stimulation guidance have no significant effect on the performance of a classifier used to distinguish between left- and right-hand MI tasks [22].

C. Decrements of Functional Connectivity

Functional connectivity reflects synchronized brain activity, allowing us to investigate the neural mechanisms involved in brain task-processing. The functional connectivity across electrodes has been suggested as a marker for communication between distant neuronal populations. At the beginning of this study, we expected the frontal-parietal connectivity during MI to be increased compared to that during resting period. However, the phase consistency across electrodes was significantly reduced during MI period compared with resting period, especially in the alpha band in the contralateral frontal-parietal network. The possible explanation of these results is that the decrements

of phase consistency might be associated with the cognitive load required in MI. Indeed, Leeuwis et al. found that functional connectivity during resting state is greater than that during MI [42]. Mylonas et al. demonstrated that phase consistency decrements at the alpha band are connected to sensorimotor integration and contribute to the improvement of motor performance [43]. Moreover, the results of this study showed that the number of alpha decoupling connectivity in post-SES block was more than that in pre-SES block. Therefore, our findings suggest that decreased phase consistency may facilitate the completion of MI tasks.

D. Limitations of Current Study

Some limitations of current study need to be mentioned. First, this study was conducted on healthy subjects. In further research, some stroke patients should be recruited to verify the generality of training based on MI+st-SES. In particular, some post-stroke patients suffer from somatosensory disorders, which may affect the effectiveness of training strategy [44]. Second, the effect of st-SES frequency was not investigated in this study. The sensations produced by the st-SES may vary depending on the stimulation frequency. Thus, further research is required to determine a more appropriate stimulation parameter. Third, only the short-term training effect was evaluated in this study. Motor-related brain patterns may be affected by the subjects' proficiency in performing MI tasks. Thus, the long-term training effect should be explored in future studies.

V. Conclusion

In this study, a training strategy combining MI and st-SES was proposed to improve the performance of MI. Our findings demonstrated that both ERD patterns and the accuracy of SVM classifiers were significantly improved following the training based on MI+st-SES. We also found that phase consistency in the frontal-parietal network decreased during MI compared to rest, and this reduction may be beneficial for performance of MI tasks. Therefore, the proposed training strategy based on MI+st-SES might be promising to optimize subject training manner and improve MI performance.

Acknowledgment

The authors sincerely thank all subjects for their voluntary participation.

References

[1] J. R. Wolpaw et al., "Brain-computer interfaces for communication and control," *Clin. Neurophysiol.*, vol. 113, no. 6, pp. 767–791, Jun. 2002.
[2] R. Foong et al., "Assessment of the efficacy of EEG-based MI-BCI with visual feedback and EEG correlates of mental fatigue for upper-limb stroke rehabilitation," *IEEE Trans. Biomed. Eng.*, vol. 67, no. 3, pp. 786–795, Mar. 2020.
[3] N. Mrachacz-Kersting et al., "Efficient neuroplasticity induction in chronic stroke patients by an associative brain-computer interface," *J. Neurophysiol.*, vol. 115, no. 3, pp. 1410–1421, Mar. 2016.
[4] G. Nelles et al., "Arm training induced brain plasticity in stroke studied with serial positron emission tomography," *Neuroimage*, vol. 13, no. 6, pp. 1146–1154, Jun. 2001.
[5] M. Jeannerod, "The representing brain: Neural correlates of motor intention and imagery," *Behav. Brain Sci.*, vol. 17, no. 2, pp. 187–202, Jun. 1994.
[6] A. Solodkin et al., "Fine modulation in network activation during motor execution and motor imagery," *Cereb. Cortex*, vol. 14, no. 11, pp. 1246–1255, Nov. 2004.
[7] G. Pfurtscheller, "Spatiotemporal ERD/ERS patterns during voluntary movement and motor imagery," *Suppl. Clin. Neurophysiol.*, vol. 53, pp. 196–198, Jan. 2000.
[8] G. Pfurtscheller et al., "Mu rhythm (de) synchronization and EEG single-trial classification of different motor imagery tasks," *Neuroimage*, vol. 31, no. 1, pp. 153–159, May 2006.
[9] C. Sannelli et al., "A large scale screening study with a SMR-based BCI: Categorization of BCI users and differences in their SMR activity," *PLoS One*, vol. 14, no. 1, Jan. 2019, Art. no. e0207351.
[10] B. Blankertz et al., "The non-invasive berlin brain–computer interface: Fast acquisition of effective performance in untrained subjects," *Neuroimage*, vol. 37, no. 2, pp. 539–550, Aug. 2007.
[11] X. Zhao et al., "A multi-branch 3D convolutional neural network for EEG-based motor imagery classification," *IEEE Trans. Neural Syst. Rehabil. Eng.*, vol. 27, no. 10, pp. 2164–2177, Oct. 2019.
[12] Y. Li et al., "A temporal-spectral-based Squeeze-and-Excitation feature fusion network for motor imagery EEG decoding," *IEEE Trans. Neural Syst. Rehabil. Eng.*, vol. 29, pp. 1534–1545, 2021.
[13] S. Ren et al., "Enhanced motor imagery based brain-computer interface via FES and VR for lower limbs," *IEEE Trans. Neural Syst. Rehabil. Eng.*, vol. 28, no. 8, pp. 1846–1855, Aug. 2020.
[14] S. Bhattacharyya, M. Clerc, and M. Hayashibe, "Augmenting motor imagery learning for brain–computer interfacing using electrical stimulation as feedback," *IEEE Trans. Med. Robot. Bionics*, vol. 1, no. 4, pp. 247–255, Nov. 2019.
[15] Z. Wang et al., "A BCI based visual-haptic neurofeedback training improves cortical activations and classification performance during motor imagery," *J. Neural Eng.*, vol. 16, no. 6, Oct. 2019, Art. no. 66012.
[16] M. Grosse-Wentrup, D. Mattia, and K. Oweiss, "Using brain–computer interfaces to induce neural plasticity and restore function," *J. Neural Eng.*, vol. 8, no. 2, Apr. 2011, Art. no. 25004.
[17] D. J. McFarland, L. M. McCane, and J. R. Wolpaw, "EEG-based communication and control: Short-term role of feedback," *IEEE Trans. Rehabil. Eng.*, vol. 6, no. 1, pp. 7–11, Mar. 1998.
[18] J. W. Choi, S. Huh, and S. Jo, "Improving performance in motor imagery BCI-based control applications via virtually embodied feedback," *Comput. Biol. Med.*, vol. 127, Dec. 2020, Art. no. 104079.
[19] F. Škola, S. Tinková, and F. Liarokapis, "Progressive training for motor imagery brain-computer interfaces using gamification and virtual reality embodiment," *Front. Hum. Neurosci.*, vol. 13, Sep. 2019, Art. no. 329.
[20] X. Shu et al., "Tactile stimulation improves sensorimotor rhythm-based BCI performance in stroke patients," *IEEE Trans. Biomed. Eng.*, vol. 66, no. 7, pp. 1987–1995, Jul. 2019.
[21] T. Corbet et al., "Sensory threshold neuromuscular electrical stimulation fosters motor imagery performance," *Neuroimage*, vol. 176, pp. 268–276, Aug. 2018.
[22] C. Vidaurre et al., "Enhancing sensorimotor BCI performance with assistive afferent activity: An online evaluation," *Neuroimage*, vol. 199, pp. 375–386, Oct. 2019.
[23] X. Zhang et al., "Alpha frequency intervention by electrical stimulation to improve performance in mu-based BCI," *IEEE Trans. Neural Syst. Rehabil. Eng.*, vol. 28, no. 6, pp. 1262–1270, Jun. 2020.
[24] L. Yao et al., "Sensory stimulation training for BCI system based on somatosensory attentional orientation," *IEEE Trans. Biomed. Eng.*, vol. 66, no. 3, pp. 640–646, Mar. 2019.
[25] M. W. Scott et al., "Combined action observation and motor imagery: An intervention to combat the neural and behavioural deficits associated with developmental coordination disorder," *Neurosci. Biobehav. Rev.*, vol. 127, pp. 638–646, Aug. 2021.
[26] F. Perrin et al., "Mapping of scalp potentials by surface spline interpolation," *Electroencephalogr. Clin. Neurophysiol.*, vol. 66, no. 1, pp. 75–81, Jan. 1987.
[27] J. Kayser and C. E. Tenke, "Principal components analysis of laplacian waveforms as a generic method for identifying ERP generator patterns: II. Adequacy of low-density estimates," *Clin. Neurophysiol.*, vol. 117, no. 2, pp. 369–380, Feb. 2006.
[28] A. Delorme and S. Makeig, "EEGLAB: An open source toolbox for analysis of single-trial EEG dynamics including independent component analysis," *J. Neurosci. Methods*, vol. 134, no. 1, pp. 9–21, Mar. 2004.
[29] J. Meng et al., "A study of the effects of electrode number and decoding algorithm on online EEG-based BCI behavioral performance," *Front. Neurosci.*, vol. 12, Apr. 2018, Art. no. 227.

[30] B. Blankertz et al., "Optimizing spatial filters for robust EEG single-trial analysis," *IEEE Signal Process. Mag.*, vol. 25, no. 1, pp. 41–56, 2008.
[31] G. Mueller-Putz et al., "Better than random: A closer look on BCI results," *Int. J. Bioelectromagn.*, vol. 10, no. 1, pp. 52–55, 2008.
[32] A. Wilsch et al., "Temporal expectation modulates the cortical dynamics of short-term memory," *J. Neurosci.*, vol. 38, no. 34, pp. 7428–7439, Aug. 2018.
[33] R. Oostenveld et al., "FieldTrip: Open source software for advanced analysis of MEG, EEG, and invasive electrophysiological data," *Comput. Intell. Neurosci.*, vol. 2011, Dec. 2011, Art. no. 156869.
[34] L. Ding et al., "Mirror visual feedback combining vibrotactile stimulation promotes embodiment perception: An electroencephalogram (EEG) pilot study," *Front. Bioeng. Biotechnol.*, vol. 8, Oct. 2020, Art. no. 1208.
[35] A. Sidarta, F. T. van Vugt, and D. J. Ostry, "Somatosensory working memory in human reinforcement-based motor learning," *J. Neurophysiol.*, vol. 120, no. 6, pp. 3275–3286, Dec. 2018.
[36] K. Stefan et al., "Induction of plasticity in the human motor cortex by paired associative stimulation," *Brain*, vol. 123, no. 3, pp. 572–584, 2000.
[37] Y. Takahashi et al., "Effects of leg motor imagery combined with electrical stimulation on plasticity of corticospinal excitability and spinal reciprocal inhibition," *Front. Neurosci.*, vol. 13, Feb. 2019, Art. no. 149.
[38] C. Babiloni et al., "Alpha, beta and gamma electrocorticographic rhythms in somatosensory, motor, premotor and prefrontal cortical areas differ in movement execution and observation in humans," *Clin. Neurophysiol.*, vol. 127, no. 1, pp. 641–654, Jan. 2016.
[39] G. Naros et al., "Reinforcement learning of self-regulated sensorimotor β-oscillations improves motor performance," *Neuroimage*, vol. 134, pp. 142–152, Jul. 2016.
[40] V. N. Buchholz, O. Jensen, and W. P. Medendorp, "Different roles of alpha and beta band oscillations in anticipatory sensorimotor gating," *Front. Hum. Neurosci.*, vol. 8, Jun. 2014, Art. no. 446.
[41] Á. Foerster et al., "Site-specific effects of mental practice combined with transcranial direct current stimulation on motor learning," *Eur. J. Neurosci.*, vol. 37, no. 5, pp. 786–794, Mar. 2013.
[42] N. Leeuwis, S. Yoon, and M. Alimardani, "Functional connectivity analysis in motor imagery brain computer interfaces," *Front. Hum. Neurosci.*, vol. 15, Oct. 2021, Art. no. 732946.
[43] D. S. Mylonas et al., "Modular patterns of phase desynchronization networks during a simple visuomotor task," *Brain Topogr*, vol. 29, no. 1, pp. 118–129, Jan. 2016.
[44] L. Pillette et al., "Why we should systematically assess, control and report somatosensory impairments in BCI-based motor rehabilitation after stroke studies," *NeuroImage Clin.*, vol. 28, Sep. 2020, Art. no. 102417.